# Instituto Superior Técnico

## Estimação e Controlo Preditivo Distribuído / Distributed Predictive Control and Estimation

## MEEC

---

### Laboratory work, P4, 2nd Semester 2022/2023

---

*Students:*
Tomás Marques Videira Fonseca | 66325 | tomas.mvf@gmail.com
Afonso Brito Caiado Alemão | 96135 | afonso.alemao@tecnico.ulisboa.pt
José Miguel Valério Antunes | 96258 | jose.m.valerio.antunes@tecnico.ulisboa.pt
Rui Pedro Canário Daniel | 96317 | ruipcdaniel@tecnico.ulisboa.pt

*Group* **2**

*Teachers:*
João Miranda Lemos, Pedro Batista

**Ethical commitment to originality**: The group of students identified above guarantees that the text of this report and all the software and results delivered were entirely carried out by the elements of the group, with a significant participation of all of them, and that no part of the work or the software and results presented was obtained from other people or sources.

June 19, 2023

# 0 Introduction

This laboratory work aims to design an MPC controller [1] to equilibrate an inverted pendulum, by deciding the design options and evaluating performance and limitations.

# 1 P4

The plant to control consists of an inverted pendulum, acted by a torque (manipulated variable), $u$, as in Fig. 1. The state of the nonlinear plant is defined by the angular position, $x_1 = \theta$, and velocity of the pendulum tip, $x_2 = \dot{\theta}$, satisfying the nonlinear model in (1), with $g = 9.8\,\mathrm{ms}^{-2}$, $L = 0.3\,\mathrm{m}$, $k = 0.01$, and $m = 0.3\,\mathrm{kg}$. Taken as equilibrium point $\theta = 0$, the state of the nonlinear model is equal to the state of the linearized model. For small deviations with respect to the equilibrium, the linearized model equations are given by (2), defined in continuous time. To obtain a model in discrete time, we used the Matlab function `c2d`.

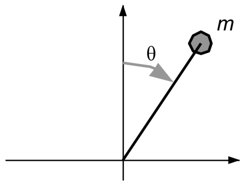


Figure 1: Plant to control.

$$\dot{x_1} = x_2 \ , \ \dot{x_2} = a \sin x_1 - b x_2 + c u \ , \ a = \frac{g}{L}, \ B = \frac{k}{m}, \ c = \frac{1}{mL^2} \tag{1}$$

$$\dot{x_1} = x_2 \ , \ \dot{x_2} = a x_1 - b x_2 + c u \tag{2}$$

The control objectives are by starting from a non-zero initial condition, acting on the torque such as to drive the angle to zero, and also such that the angle tracks a reference of small amplitude.

## 1.1

By adapting the examples in P3, we simulate the control of the nonlinear inverted pendulum with MPCtools 1.0 [2], using the code in `P4.m` and the Simulink diagram in `Pendulum.slx` (Fig. 2). The MPC controller is based on a linearized, discrete-time model, but the simulation tests are made with a nonlinear, continuous time, model, so it is required to use a Zero-Order Hold (ZOH) between the plant and the controller, as in Fig. 2(a), to convert the continuous signal into a discrete one, with $h$ as sampling interval. The nonlinear plant in (1) is simulated in the red block, detailed in Fig. 2(b), where the initial condition for $\theta$ is given by $\theta_0$. In these figures, the presence of disturbances in the system is represented, which will be discussed in more detail in 1.4 where the subsystem "Disturbance Generator" will be presented. In sections 1.2 and 1.3, we do not consider the presence of disturbances, i.e., `flagdist`$= 0$.

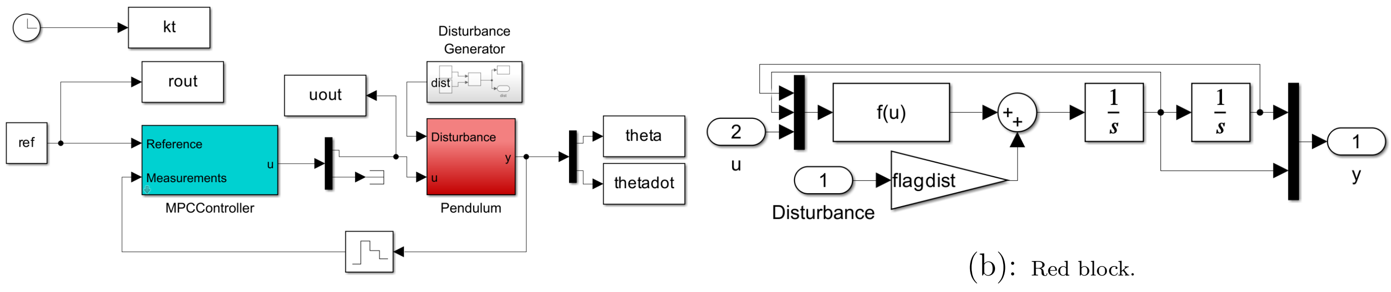


(a): General view.

(b): Red block.

Figure 2: Simulink block diagram to simulate the pendulum control.

## 1.2

In this question, we obtained an ideal configuration of the MPC parameters, based on a chosen merit figure, $M_f$, given by (3), with the constraints $|u| \leq u_{lim}$, $|\Delta u| \leq \Delta u_{lim}$, and $\theta_{lim_{min}} \leq \theta \leq \theta_{lim_{max}}$, and $S$ as the absolute value of the overshoot/undershoot. We use $Q = 1$, $\theta_0 = \frac{\pi}{8}$ rad and $\theta_{lim} = 10000$ rad.

In the design of $M_f$, we considered that it should be representative of the system performance (and of the quality of the response): the better the performance of the controller, the higher $M_f$. The faster the system converges, the smaller it is $t_{conv_{\pi/360}}$ (time instant the system converges to the reference at a margin of $\pi/360$ rad), so $M_f$ should decrease with $t_{conv_{\pi/360}}$. A higher $S$ means lower performance, so $M_f$ should decrease with $S$. We use the term $S + 0.1$ to avoid that $S \to 0$ leads to $M_f \to \infty$. With the increase of

$H_p$ and with the decrease of $h$ the system becomes computationally heavier, so $M_f$ should decrease with $H_p$ and increase with $h$. As in P3, $Q$ is the weight for minimizing the error between the output and the reference, and $R$ is the weight for minimizing the energy of $\Delta u$, so $M_f$ should increase with $R/Q$ to reward the energy efficiency of the system. For the energetic reason and to take into account the limitations of real systems in the control signal and in its variation, $M_f$ should decrease with $u_{lim}$ and with $\Delta u_{lim}$.

$$M_f = \frac{R\,h}{Q\;t_{conv_{\pi/360}}\;H_p\;(S+0.1)\;u_{lim}\;\Delta u_{lim}} \tag{3}$$

We perform the tuning of the following parameters: $\{H_p, \frac{Q}{R}, u_{lim}, \Delta u_{lim}, h\}$. As default values we consider: $H_p = 3, \frac{Q}{R} = 1000$ $(R = 0.001)$, $u_{lim} = 100\,\text{Nm}$, $\Delta u_{lim} = 100\,\text{Nm}$, and $h = 0.1\,\text{s}$. Then, for each of these, we vary the parameter, keeping those not tuned yet as default and the remaining with the tuned values. We follow the tuning order represented in the subfigures of Fig. 3. The range of variation of each parameter is represented by the range of values on the $x$-axis of each plot and was chosen so that the maximum of $M_f$ is shown and it only includes cases where $\theta$ converges to 0. We report in Fig. 3 plots of $M_f$ in function of each one of the tuning parameters, with the goal of tune them by maximization of $M_f$. The code used is in `P4_tuning.m`.

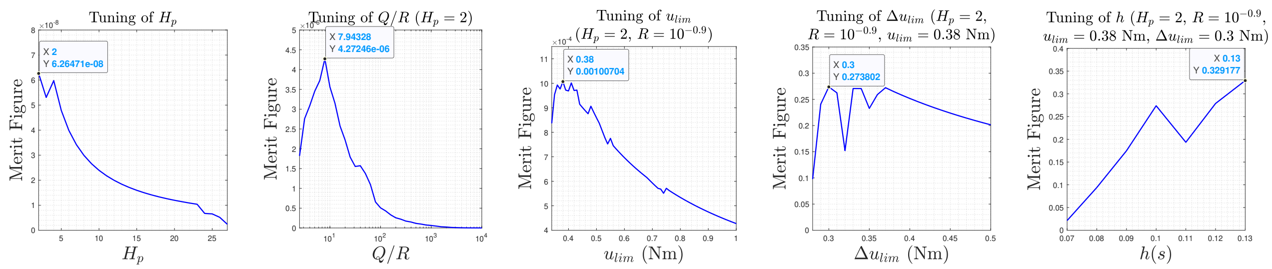


(a): $H_p$. (b): $\frac{Q}{R}$. (c): $u_{lim}$. (d): $\Delta u_{lim}$. (e): $h$.

Figure 3: Merit figure in function of different tuning parameters.

In each figure is represented the value of each parameter that maximizes $M_f$: $H_p = 2$, $\frac{Q}{R} \approx 7.943$ $(R = 10^{-0.9} \approx 0.126)$, $u_{lim} = 0.38\,\text{Nm}$, $\Delta u_{lim} = 0.3\,\text{Nm}$, $h = 0.13\,\text{s}$. So, we choose this configuration of the MPC parameters and report its results in Fig. 4. The code used is in `P4_2.m`. The convergence of $\theta$ to the reference is fast (low $t_{conv_{\pi/360}}$), with low $S$, low $H_p$ and reasonably high $h$ (low computational load), a very strict constraint for $u$ and $\Delta u$, and $Q/R$ that guarantees the goal of minimizing the energy of $\Delta u$ in addition to the follow-up of the reference.

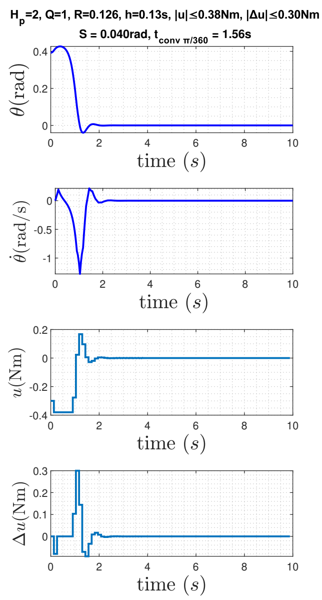


Figure 4: MPC control with tuned parameters.

## 1.3

In order to discuss the limitations imposed by hard-limiting the control action, we simulate the pendulum control with MPC, illustrating the effect of constraints on the control action and on its variation, and the effect of enlarging the horizon, $H_p$. With the choice $H_w = 1$ and $H_u = H_p = H$, the cost function is quadratic, given by (4), where the time increments $\Delta u = u(k) - u(k-1)$ are penalized. The considered default values were $\theta_0 = \frac{\pi}{8}$ rad, $|u| \leq 100\,\text{Nm}$, $|\Delta u| \leq 100\,\text{Nm}$, $\theta_{lim_{max}} = 10000$ rad, $\theta_{lim_{min}} = -10000$ rad, $R = 0.001$, $Q = 1$, $H = 3$, and $h = 0.1\,\text{s}$. The results obtained by varying the controller constraints (using the default in the remaining parameters) are reported in Fig. 5 and by varying $H$ in Table 1.

$$J(k) = \sum_{i=1}^{H} \|\hat{\theta}(k+i|k) - r(k+1|k)\|_Q^2 + \sum_{i=0}^{H-1} \|\Delta\hat{u}(k+i|k)\|_R^2\,,\ \text{with}\ \|v\|_M^2 = v^T M v \tag{4}$$

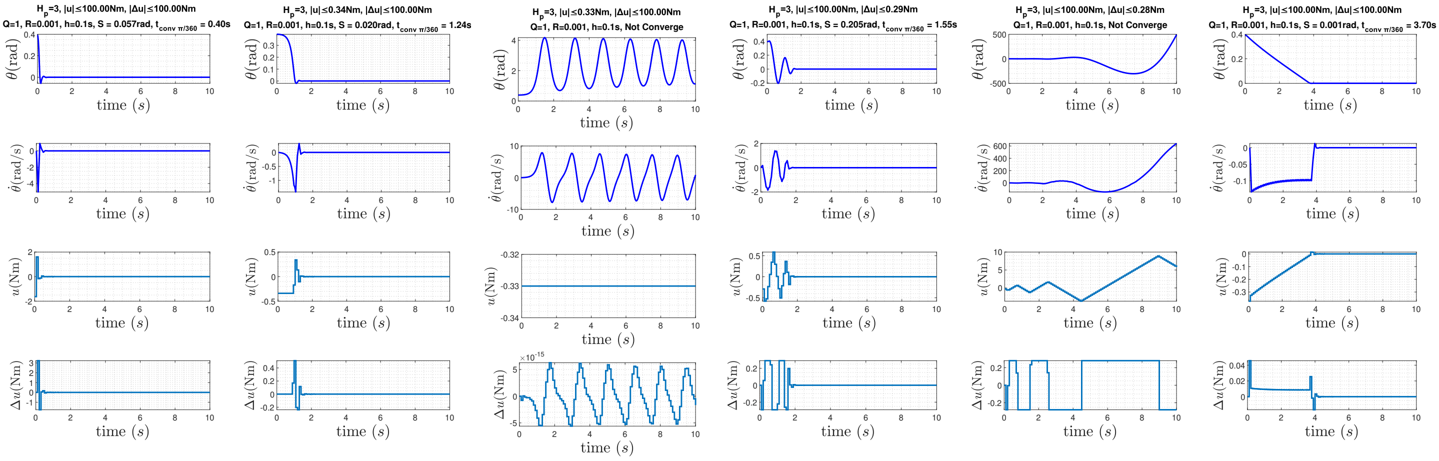

(a): Default. (b): $u_{lim} = 0.34\,\text{Nm}$. (c): $u_{lim} = 0.33\,\text{Nm}$. (d): $\Delta u_{lim} = 0.29\,\text{Nm}$. (e): $\Delta u_{lim} = 0.28\,\text{Nm}$. (f): $\theta_{lim_{min}} = -0.1$.

Figure 5: MPC pendulum control varying constraints.

With a constraint on $|u|$ or on $|\Delta u|$, the stricter the constraint, in cases that $\theta$ converges to the reference, usually this convergence is slower, as in Fig. 5(b) and Fig. 5(d).

If $u_{lim}$ or $\Delta u_{lim}$ is sufficiently small, $\theta$ may not converge to 0 (e.g., $u_{lim} = 0.33\,\text{Nm}$ in Fig. 5(c), and $\Delta u_{lim} = 0.28\,\text{Nm}$ in Fig. 5(e)), because we are restricting the energy of $u$ or of $\Delta u$ which has a similar effect of increasing $R$ due to (4). In the last case, it is necessary to increase $H$ in order to guarantee convergence to 0.

Table 1: Response characteristics of MPC pendulum control varying $H$.

Fig. 5(a)

| $H$ | $S$(rad) | $t_{conv_{\pi/360}}(s)$ |
|---|---|---|
| 2 | 0.102 | 0.39 |
| 3 | 0.057 | 0.40 |
| 4 | 0.057 | 0.27 |
| 5 | 0.056 | 0.27 |
| | ... | |

Fig. 5(b)

| $H$ | $S$(rad) | $t_{conv_{\pi/360}}(s)$ |
|---|---|---|
| 2 | 0.018 | 1.20 |
| 3 | 0.020 | 1.24 |
| | ... | |

Fig. 5(c)

| $H$ | $S$(rad) | $t_{conv_{\pi/360}}(s)$ |
|---|---|---|
| 2 | Not Converge | |
| | ... | |
| 23 | Not Converge | |

Fig. 5(d)

| $H$ | $S$(rad) | $t_{conv_{\pi/360}}(s)$ |
|---|---|---|
| 2 | Not Converge | |
| 3 | 0.205 | 1.55 |
| 4 | 0.050 | 0.74 |
| 5 | 0.055 | 0.74 |
| | ... | |

Fig. 5(e)

| $H$ | $S$(rad) | $t_{conv_{\pi/360}}(s)$ |
|---|---|---|
| 2 | Not Converge | |
| 3 | Not Converge | |
| 4 | 0.066 | 0.90 |
| 5 | 0.089 | 0.94 |
| | ... | |

Fig. 5(f)

| $H$ | $S$(rad) | $t_{conv_{\pi/360}}(s)$ |
|---|---|---|
| 2 | 0.001 | 3.70 |
| 3 | 0.001 | 3.70 |
| | ... | |

In the default configuration, for $H \geq 2$, $\theta$ converges to 0. For $2 \leq H \leq 4$, by increasing $H$, that convergence has lower $S$ and smaller oscillations. For $H \geq 4$ the increase of $H$ may not represent an improvement in performance and the computational load increases.

With the constraint $u_{lim} = 0.34\,\text{Nm}$, for $H \geq 2$, the convergence is fast, with low $S$ and small oscillations. However, the increase of $H$ may not represent an improvement in performance. With the constraint $u_{lim} = 0.33\,\text{Nm}$, for the tested range of $2 \leq H \leq 23$, $\theta$ does not converge to 0.

For the constraints tested on $\Delta u$, for $H \leq H_1$, $\theta$ does not converge to 0, with $H_1 = 2$ for $\Delta u_{lim} = 0.29\,\text{Nm}$, and $H_1 = 3$ for $\Delta u_{lim} = 0.28\,\text{Nm}$. For $\Delta u_{lim} = 0.29\,\text{Nm}$, in $3 \leq H \leq 4$, by increasing $H$, the convergence becomes faster, with lower $S$ and smaller oscillations. For $H \geq 4$, in both cases, the system converges, but the increase of $H$ may not represent an improvement in performance.

With the constraint $\theta_{lim_{min}} = -0.1\,\text{rad}$ (Fig. 5(f)), for $H \geq 2$, the convergence is slow, with low $S$ and small oscillations, and the increase of $H$ may not represent an improvement in performance.

In LQ control, it is considered an infinite horizon. We also simulate the pendulum control with LQ, illustrating the effect of constraints on the control action. Using $R = 0.001$, $Q = 1$, $\theta_0 = \frac{\pi}{8}$ rad and varying $u_{lim}$, the obtained results are reported in Fig. 6. The LQ control cannot deal with constraints by design, so the control action limitation is included through a saturation block.

As it is for MPC control, in LQ control $\theta$ converges to 0 for $u_{lim} \geq 0.34\,\text{Nm}$ (e.g, Fig. 6(b)) and does not converge to it for $u_{lim} \leq 0.33\,\text{Nm}$ (e.g, Fig. 6(c)), in the studied configuration. However, by comparing Fig. 6(a) with Fig. 5(a) and Fig. 6(b) with Fig. 5(b), we can verify that for the LQ control, the convergence is slower, with lower $S$ and smaller oscillations.

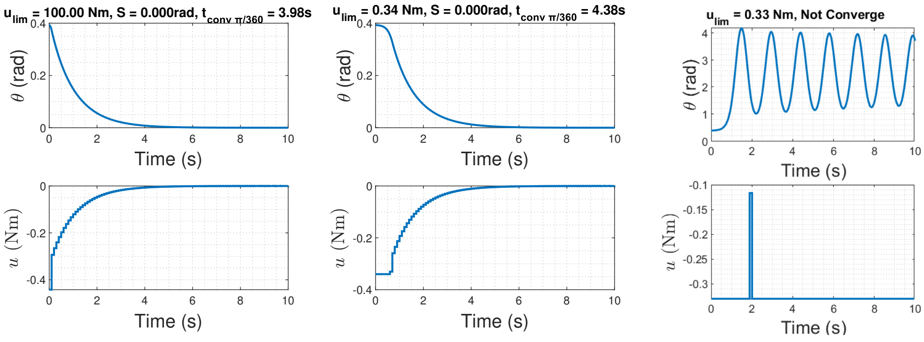


(a): $u_{lim} = 100\,\mathrm{Nm}$. (b): $u_{lim} = 0.34\,\mathrm{Nm}$. (c): $u_{lim} = 0.33\,\mathrm{Nm}$.

Figure 6: LQ pendulum control varying $u_{lim}$.

Then, we consider a situation in which the pendulum starts with some inclination $\theta_0$, and with the control constraints $u_{lim} = 0.3\,\mathrm{Nm}$ and $\Delta u_{lim} = 0.2\,\mathrm{Nm}$. We simulate the pendulum control with MPC, illustrating the effect of each $\theta_0 \in ]-\pi;\pi]$ rad, in the code `P4_3_convergence_region.m`. From there, we obtain that the system converges in $t < 10\,\mathrm{s}$ for $|\theta_0| \leq 0.285\,\mathrm{rad} = \theta_t$ (basin of attraction), using $|\theta| \leq 10000$ rad, $R = 10^{-0.9}$, $Q = 1$, $h = 0.13\,\mathrm{s}$ and $H = 3$. We report the obtained results by varying $\theta_0$ in terms of performance characteristics ($t_{conv_{\pi/360}}$, $S$) in Fig. 7.

When the initial angle, $\theta_0$, deviates more with respect to the vertical, i.e, when $|\theta_0|$ (in the range $|\theta_0| \leq 0.285\,\mathrm{rad}$) increases, usually the convergence becomes slower (higher $t_{conv_{\pi/360}}$) and with higher $S$.

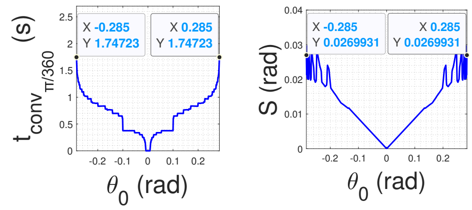


(a): $t_{conv_{\pi/360}}$. (b): $S$.

Figure 7: Response quality in function of $\theta_0$.

## 1.4

In this question, we study the effect of disturbances. In Fig. 2 we already present the disturbances in the system. Now, we consider their presence, i.e., `flagdist`$= 1$. The "Disturbance Generator" subsystem is represented in Fig. 8(a). We use a sine wave with period $T = 0.5\,\mathrm{s}$ and amplitude $A_d$, and a square wave that in the time range considered ($t \in [0; 10]$ s) is only equal to 1 in $t \in [5; 5.5]$ s, and otherwise is equal to 0. By multiplying them, we obtain the disturbance in Fig. 8(b), where $A_d = 8.5\,\mathrm{rad\,s^{-2}}$. In Fig. 2, the disturbance is added to the $\dot{x_2} = \ddot{\theta}$ term of (2), because it is an angular acceleration with units $\mathrm{rad\,s^{-2}}$.

Using the configuration of MPC tuned parameters of section 1.2, $H = 2$, $Q = 1$, $R = 10^{-0.9}$, $u_{lim} = 0.38\,\mathrm{Nm}$, $\Delta u_{lim} = 0.3\,\mathrm{Nm}$, $h = 0.13\,\mathrm{s}$, and $\theta_0 = \frac{\pi}{8}$ rad, we report in Fig. 9 the obtained results of the effect of a disturbance for $A_d = 8.5\,\mathrm{rad\,s^{-2}}$ and for $A_d = 8.6\,\mathrm{rad\,s^{-2}}$. In these, we verify that for $A_d = 8.5\,\mathrm{rad\,s^{-2}}$ the system is able to reject the disturbance and $\theta$ converges back to the reference, and for $A_d = 8.6\,\mathrm{rad\,s^{-2}}$, from the instant the disturbance occurs, $\theta$ does not converge to the reference.

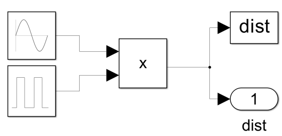


(a): Simulink block diagram.

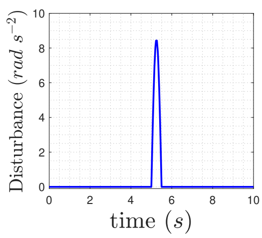


(b): Plot with $A_d = 8.5\,\mathrm{rad\,s^{-2}}$.

Figure 8: Disturbance simulation.

The disturbance simulates a wind gust, in which the wind pressure evolves, in a deterministic way, causing the increase of $\theta$, which makes the MPC controller act more significantly on the system to make $\theta$ converge back to the reference. Depending on the MPC parameters and on $A_d$, the system may or may not be able to reject the disturbance.

In the studied configuration, the system is able to reject the disturbance, converging to the reference for $A_d \leq A_t$, with $A_t \approx 8.5\,\mathrm{rad\,s^{-2}}$, and for values of $A_d$ higher than $A_t$, the system is no longer able to reject the disturbance, not converging to the reference.

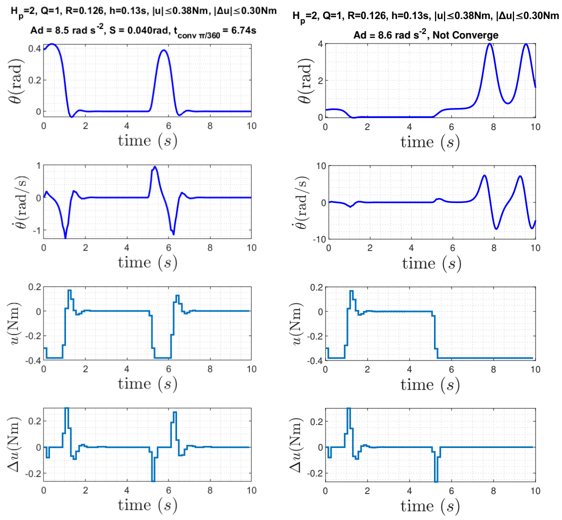


(a): $A_d = 8.5\,\mathrm{rad\,s^{-2}}$. (b): $A_d = 8.6\,\mathrm{rad\,s^{-2}}$.

Figure 9: MPC pendulum control using tuned parameters and varying $A_d$.

# 2 Track square wave

As requested in the control objectives, we also act on $u$ such that the angle tracks a reference of small amplitude, in this case, a square wave with $T = 10\,\mathrm{s}$ and amplitude equal to $\frac{\pi}{180}$ rad.

We performed MPC control using 2 different parameter configurations: the default values, and the tuned values (with $h = 0.1\,\mathrm{s}$), both of section 1.2. Using $\theta_0 = \frac{\pi}{180}$ rad, the results obtained are reported in Fig. 10. The code used is in `Pextra.m` and the Simulink model in `Pendulum_extra.slx`.

With both these MPC configurations, $\theta$ follows the reference with fast convergence, low $S$, and small oscillations. The quickness of the convergence was analyzed by the time instant the system converges to the reference at a margin of 5% of the final value, $t_{conv0.05}$.

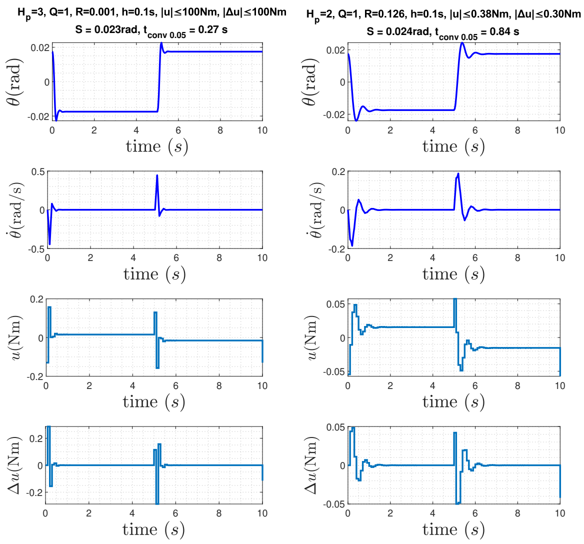


(a): Default configuration. (b): Tuned configuration.

Figure 10: MPC pendulum control of square wave.

# 3 Conclusion

We design an MPC controller for the inverted pendulum. We choose a merit figure to tune its parameters that guarantee the convergence to the reference quickly, with low $S$, in an energy-efficient way, with low computational load, and considering constraints on $u$ and $\Delta u$ (real world limitations). We also studied how $\theta_0$ and $A_d$ can affect the system's response. For $|\theta_0| > \theta_t$ and for $A_d > A_t$, $\theta$ does not converge to the reference. The larger $\theta_t$, the better the capacity of the system to handle higher values of $\theta_0$, and the larger $A_t$, the better the capacity of the system to handle disturbances. Thus, the parameters $A_t$ and $\theta_t$ should have been incorporated into the merit figure which should increase with them.

# References

[1] Distributed Predictive Control and Estimation (ECPD) Slides - Slides of Theoretical Classes 2022/2023, 2nd Semester (MEEC), by João Miranda Lemos;

[2] ECPD 2022/2023, Laboratory Work, by João Miranda Lemos.